NATURAL RESOURCES PROGRAM

SPACE APPLICATIONS PROGRAMS

[redacted]

U.S. Government Agencies and Contractors Only

TECHNICAL LETTER NASA-18

U. S. Government Agencies and Contractors Only

U.S. Government Agencies and Contractors Only

U.S. Geological Survey
Department of the Interior

A MILLIMETER WAVELENGTH INTERFEROMETER SPECTROMETER

BY

GEERT WYNTJES

AND

NEILS O. YOUNG

FINAL REPORT

CONTRACT 13009

PREPARED FOR:

U. S. Geological Survey #13009

Branch of Theoretical Geophysics
Room 1243, GS Bldg.
Washington, D.C.

SUBMITTED BY:

Block Engineering, Inc.
19 Blackstone Street
Cambridge, Massachusetts

TABLE OF CONTENTS

I. INTRODUCTION

Under this study program, a millimeter wavelength interferometer spectrometer for geological measurements has been designed and theoretically evaluated. The primary motivation for the development of an optical instrument operating in the millimeter wavelength region is to obtain wide spectral coverage; available microwave receivers limit measurements to narrow spectral bands.

The interferometer spectrometer, described in the following, scans the .5mm to 2mm wavelength region at a rate of 2 scans/sec, has a maximum resolution of .05cm^{-1}, and achieves, for a 300°k blackbody source filling the f.o.v. and an emissivity of .1, a S/N per resolution element of $\approx$150. The instrument, called the Bipath Interferometer Spectrometer, has a cryogenic detector and provisions for cryogenically cooling the optical system.

Block Engineering is confident that fabrication of the bipath interferometer spectrometer is feasible and that the specifications cited on page 7 of this report can be realized in an operational instrument. It is felt that the Bipath Interferometer Spectrometer will be a particularly useful instrument for broadband spectral studies, such as atmospheric absorption measurements, terrestial studies, and extraterrestial emission measurements. Equipped with a cold-sample holder, the bipath interferometer spectrometer would also be useful for material studies.

The instrument is compact in size, low in weight, and has relatively good tolerance to vibration. These features, together with a conventional data form suitable for telemetry, will enable the interferometer to be used for airborne, rocket-borne and satelliteborne applications, in addition to field measurements.

II. OPTICAL VS. MICROWAVE TECHNIQUES

The millimeter wave region is the region where optical techniques from the infrared and microwave techniques extended from the centimeter wave region meet. For radiometric measurements in the 0.5mm to 2mm region a decision should be made either to use microwave techniques or to use an infrared approach. In general this decision can be made on the basis of the spectral bandwidth. In the case where the source emits energy over a narrow spectral region, e.g. resonance lines, a microwave receiver, because of its higher sensitivity and narrow bandwidth, is to be preferred. However, when the source emits radiation as a black or grey body, the narrow-band receiver will not necessarily give the best signal-to-noise ratio, S/N. This is shown in the following example.

Assume a super heterodyne receiver used as a "Dicke Radiometer" operating at 1mm. with a bandwidth, BW = 100 Mc; a noise temperature, T = 100,000°K; an output bandwidth, $\Delta f = 1$ cps. This receiver will give a minimum power sensitivity of 2×10^{-14} watts. A blackbody at 300°K will have a power output over the 100 Mc bandwidth at 1mm of $P_{\Delta f = 100\ Mc} = 8.5 \times 10^{-11}$ watts. Under these conditions, the S/N of the receiver is $\frac{8.5 \times 10^{-11}}{2 \times 10^{-14}} = 42.5$.

For comparison, an interferometer spectrometer with a resolution of .05 cm^{-1} could accept a maximum power per resolution element of 1.3×10^{-11} watts. A direct detector having a minimum power sensitivity of 10^{-13} watts at 1mm may be used with the interferometer. The S/N of the interferometer system is then

$$\frac{1.3 \times 10^{-11}}{10^{-13}} = 130.$$

Since considerations of field-of-view, detector size, etc., have been ignored in this example, the calculations only show relative values. However, the calculations do show that with equivalent collecting systems the S/N is approximately the same.

The interferometer spectrometer has many features which will make it a useful alternate instrument to the microwave receiver. Among these are the following:

A. Wide Spectral Coverage - This wide spectral coverage does not entail a loss in S/N per spectral resolution element, as would be the case for a tunable microwave receiver or a dispersive type optical instrument. Since the detector noise is independent of radiation flux, for the same total observation time the interferometer will have a gain of $\sqrt{n}$ in S/N, where n is the number of resolution elements. (Fellgett's Advantage)

B. Throughput - Unlike dispersive instruments which employ slits and gratings, the interferometer has a large entrance aperture which permits much more energy to be gathered.

C. Adjustable Resolution

D. Compact size and low weight

E. The interferometer may be easily modified to accomodate different wavelength regions.

Admittedly, the future availability of microwave local oscillators, tunable over a wide band, low conversion loss mixers and I.F. strips equipped with travelling wave tubes could change the situation. However, this instrumentation would of necessity be much more complex, larger, heavier, and more expensive than the interferometer spectrometer.

III. THE BIPATH INTERFEROMETER SPECTROMETER

The optical cube of the bipath interferometer is drawn to full scale in Figure 1. In the drawing, the entrance and detector legs are metal light pipes which serve to collimate the radiation; S is a beamsplitter; M_1 and M_2 are stationary spherical mirrors, and M_3 is a double surfaced movable mirror.

3.1 Theory of Operation

The interferometer codes the incident radiation by means of the constructive and destructive interference of light waves.

The function of the optical cube is to heterodyne the extremely high electromagnetic frequencies of the incident radiation down to audio frequencies which the detector can follow. The audio frequencies on the detector are an exact analog of the original light frequencies since the frequency transformation which takes place in the interferometer is linear.

Optical ray traces of the bipath interferometer are shown in Figure 1. The beamsplitter, S, is a semi-reflective mirror which reflects 50% of the light which strikes it and permits the other 50% to pass. The stationary mirrors M_1 and M_2 as well as the moving mirror M_3 reflect all the light which reaches them.

If a light beam enters as shown, 50% of it will pass

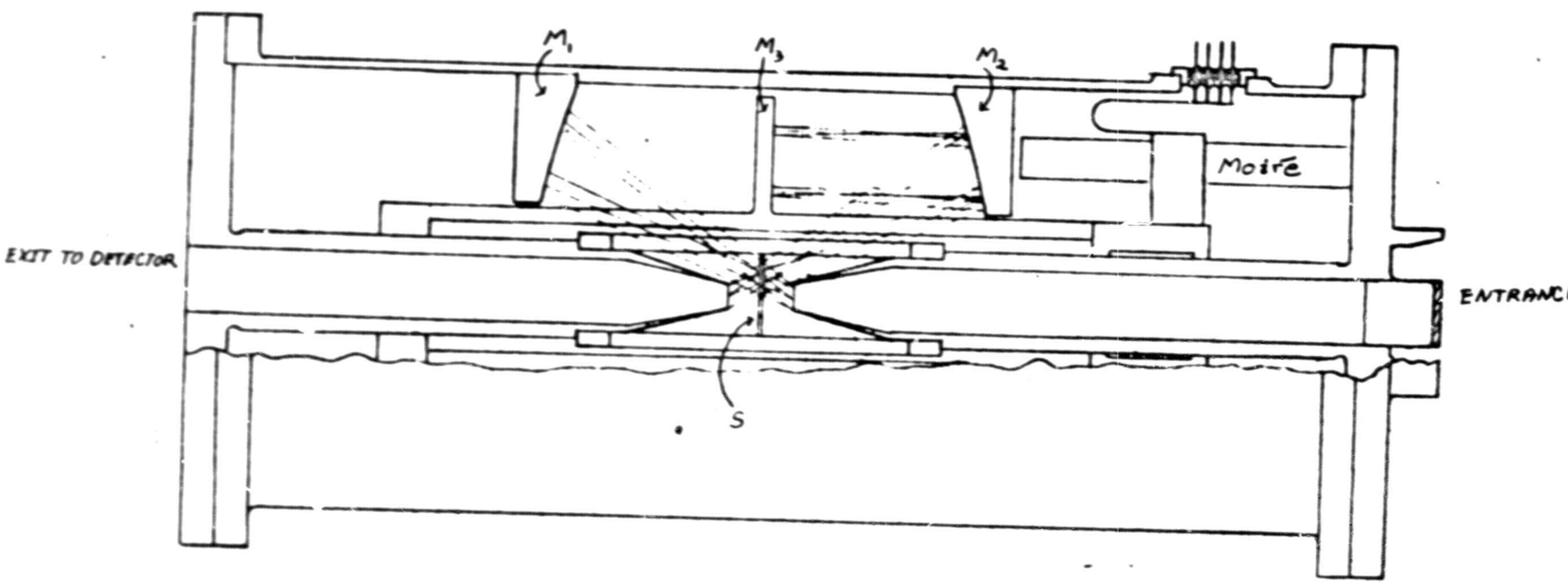

.5 - 4 mm INTERFEROMETER, x1

FIGURE 1.

NAY 21-I-66

through the beamsplitter and continue toward M_1 while the other 50% will be reflected toward M_2. Upon reaching mirrors M_1 and M_2, each fractional half of the original energy will be completely reflected to mirror M_3, then back again to mirror M_1 (or M_2) where it is reflected toward the beamsplitter. Upon reaching the beamsplitter for the second time, light traveling the M_1 path is reflected whereas that traveling the M_2 path is transmitted by the beamsplitter to the light pipe leading to the detector. The portion of light transmitted to the detector and the portion of light lost from the interferometer depends on the relative phases of the recombined rays in the detector leg of the interferometer. Since the sum of the phase shifts caused by reflections and transmission is the same for both paths, the relative phases of the recombined rays depends only on the path lengths.

For zero retardation (equal optical path lengths), all of the original light which reaches the detector via path M_1 is in phase with that arriving via path M_2, thus producing a bright central fringe on the detector. If, however, we cause the M_3 mirror to be displaced an amount Δx, we find that the phase of the light arriving at the detector via route M_1 is retarded by an amount $4\Delta x$ from that arriving via route M_2. For monochromatic light of wavelength λ, a displacement $\Delta x = \lambda/8$ will cause a retardation of $4x = 4\lambda/8 = \lambda/2$. The two equal amplitude light fractions will therefore reach the detector an increment of π out of phase, cancellation will result, and the net signal of wavelength λ to the detector will be zero. The detector signal will, in fact, be zero for all displacements Δx which are odd multiples of $\lambda/8$ ($\pm\ \lambda/8$, $\pm\ 3\ \lambda/8$, $\pm\ 5\ \lambda/8$, etc.) and will be equal to the total input energy (minus absorptions) for all even multiples of $\lambda/8$ beginning with zero (0, $\pm\ \lambda/4$, $\pm\ \lambda/2$ $\pm\ \lambda$, etc.), where the plus and minus signs denote displacements on both sides of zero retardation corresponding to increased or decreased optical path lengths (retardations) respectively.

If the displacement of mirror M_3 is slowly changed, we find that the energy at the detector goes through a series of maxima and minima (light and dark "fringes") as the retardation of the optical path lengths of the two legs differs by integral numbers of wavelengths, according to the expression

$$I = 0.5\ I_o \quad (1 + \cos 2\pi \nu Bt/T) \qquad (1)$$

where ν is the wavenumber of the incident radiation in cm^{-1}, and $Bt/4T$ is the instantaneous displacement, x, of the mirror moving a distance B/4 in time T. In other words, the frequency of the energy transmitted to the detector is a joint function of the wavenumber of the input radiation and the mirror velocity B/4T.

Since the optical retardation, B, is four times the mirror displacement, then,

$$f_\nu = 4 \cdot \nu \cdot \frac{B}{4T} = \nu \cdot \frac{B}{T} \qquad (2)$$

Increased mirror velocity yields higher output frequencies.

The detector signal for incident radiation of only one wavelength is a simple cosine wave. For incident radiation composed of many wavelengths, the signal is a complex one called an "interferogram"; since all of the wavelengths are processed simultaneously, an interferogram is the superposition of all of the cosine waves that would have been generated had each of the incident wavelengths been processed separately. The interferogram is, in fact, the Fourier transform of the incident radiation into the time-amplitude domain. The interferogram is then converted to the amplitude-frequency domain, or spectrum, by means of an inverse Fourier transform. Data processing of interferograms is discussed in Section VII of this report.

3.2 COLLECTED SPECIFICATIONS

Bipath Interferometer

Spectral Range:	0.5mm to 2mm (20 cm^{-1} to 5 cm^{-1}; 600Gc to 150Gc)
Resolution:	Adjustable to a maximum of .05 cm^{-1} ($\frac{\lambda}{\Delta\lambda}$ = 400; 1.5Gc)
Scan Rate:	2 scans/sec.
Detector:	InSb ("Rollin" detector) cooled to 4.3° K
Detector N.E.P.:	6 x 10^{-13} watts
Throughput θ :	0.2 ster - cm^2
Collecting Efficiency:	30%
Modulation Efficiency:	30%
N.E.S.R.	3 x 10^{-10} watts/ster-cm^2 f r a 1 sec. observation time.
S/N per resolution element:	≈150 for a 300° K blackbody filling the field-of-view.
Cooling:	Detector - liquid helium Optics - liquid nitrogen
Observation Time:	Depends on source stability
Output:	Analog signal and Moiré signal
Weight:	Approximately 30 lbs.
Dimensions:	Cylindrical; diameter 8", height 32"
Power Requirements:	Approximately 30 watts
Field-of-view:	± 5°
Data Reduction:	Analog or digital

3.3 The Optical System

Transmitting Components

As a minimum, one transmission component is required -- the beamsplitter. Although beamsplitters made of polyethylene, with or without a germanium coating, are more commonly used in the long wavelength region, we have chosen to use crystal quartz because this material permits greater accuracy of manufacture. The beamsplitter, being of small dimensions compared with the other interferometer components, is easily replaced for such modifications as may be dictated by experiment. Likewise, if experiments should reveal the need for optical elements in the input optics, these would also be made of crystal quartz.

Throughput

Throughput is a description of the capacity of an optical system to transmit power. Throughput, Θ, is given by:

$$\Theta = (\tfrac{1}{2}\,\pi\, D \sin\alpha)^2$$

where D is the diameter of an aperture in the system where the convergence half-angle α is the same at all points. In the bipath interferometer, the half-angle at the light pipe entry toward the beamsplitter lies between 23 and 33 angular degrees; resulting in a solid angle of 0.5 steradian. The diameter of the light pipe entry is 0.20 inches, corresponding to an area of 0.20 cm^2. The resulting throughput, to be conserved by suitable matching optics is 0.2 ster-cm^2.

Resolution

The capability of the instrument to resolve two neighboring frequencies is specified in terms of the smallest increment of wavelength, $\Delta\lambda$, which can be distinguished at the output (or alternatively, in terms of wavenumber, $\Delta\nu$). The limit of spectral resolution is a constant dependent only on the maximum internal retardation, B, according to $\Delta\nu = k/B$ where k is determined by the amount of refraction at the entrance aperture. For the proposed instrument, k = 1, approximately. Thus, for a maximum resolution $\Delta\nu$ of .05 cm^{-1} a peak retardation, B, of 20 cm is required. The resolution may be adjusted to any desired lower value by simply decreasing the retardation.

Mirror Drive Mechanism

The movable mirror of the interferometer is mounted on the armature of an electromagnet and is displaced by changing the d.c. current through the armature. Requirements for parallelism of the mirror motion are not severe in the long wave-length region. Therefore, conventional "off the shelf" bearings will be used for parallel motion rather than spring strip assemblies or special bearings. Since the position of the component which introduces retardation must be known within a fraction of a wavelength, a Moiré fringe counter is employed to keep track of the location of the moving mirror. The Moiré fringe counter is described in the following subsection.

Figure 2 is a plot of the mirror motion in time showing the linear mirror displacement. The mirror will be driven through two complete excursions a second. Because inertial effects vary as the square of the throw, the interferometer is designed to produce a retardation of 20 cm with a minimum mirror throw; the throw required is 5 cm peak to peak. This amounts to a mirror velocity which is high compared to that of the interferometers operating at shorter wavelengths. To achieve high velocities easily, the drive mechanism should be maintained at room temperature, and may have a Moiré counter in addition to the one on the interferometer

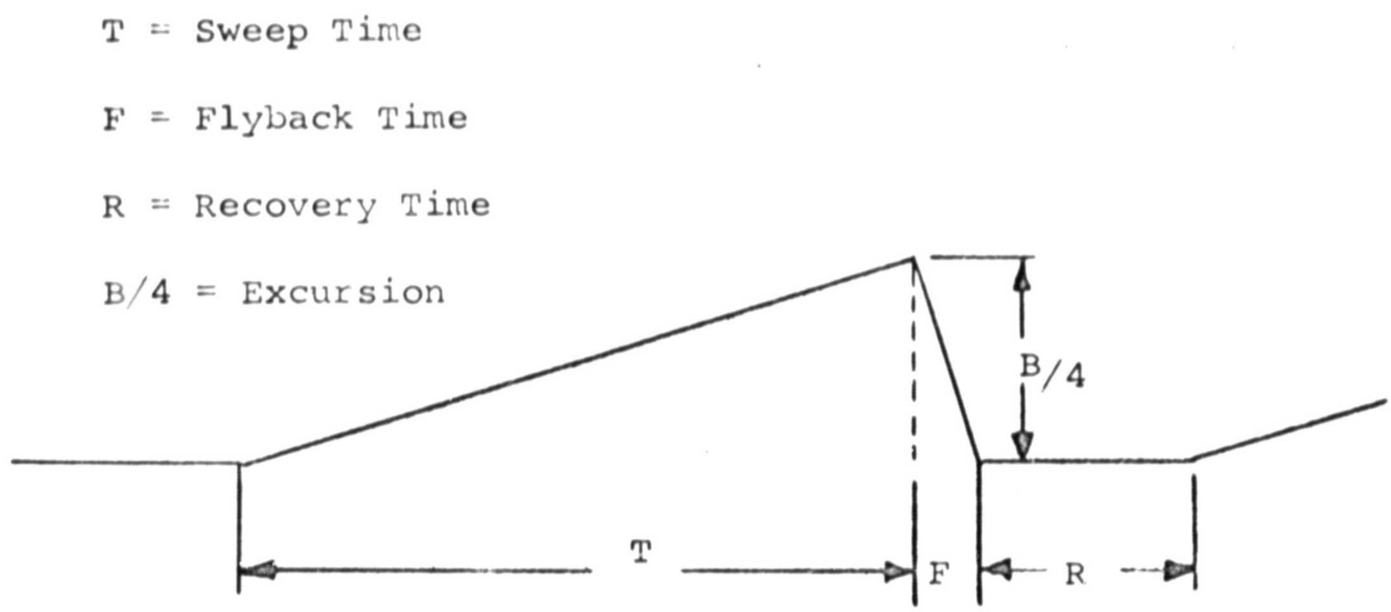

Mirror Motion

FIGURE 2.

The Moiré Fringe Counter

The Moiré fringe counter consists of two matched gratings placed very close together with a large number of lines per inch, with the width of the lines equal to the spacing between them. As one grating is moved slowly across the other with the direction of motion perpendicular to the grating lines, the two sets of lines first coincide perfectly, then less and less until the lines of one grating fill the spaces of the other. The light transmitted through the pair correspondingly varies from a maximum value of half of the incident light less transmission losses to a minimum value of zero. If the motion is uniform the transmission function will be a triangle wave with equal periods. If the motion is not uniform the transmission function will be a triangle wave with varying periods.

In the bipath interferometer, one grating is rigidly fixed to the mounting of the movable mirror. The other grating is placed between a light source and the first grating. On the other side of the first grating is a detector. As the mirror and fixed grating move, the variation of the light intensity is picked up and amplified by the detector. The position of the mirror at any time can thus be known to an accuracy of at least 1/Nth of an inch, where the grating has N lines per inch, by observing the Moiré fringe pattern.

In this way the precise position of the mirror can be monitored during the time of its scan. By simultaneously monitoring the fringe pattern and the interferogram, distortions in the interferograms caused by non-uniformities of the mirror motion can be corrected.

IV. Detector

4.1 Selection

For the spectral region from .5 mm to 2 mm, the following detectors are available: The Golay cell, the Putley detector; the germanium bolometer; and the "Rollin" detector. The last three require cooling to liquid helium temperature. Considering factors like sensitivity, time constant, and detectivity, the "Rollin" detector appears to be the best choice in this spectral region.[1]

The "Rollin" detector has the highest reported detectivity in the mm wave region. The short time constant of the "Rollin" detector ($\sim 10^{-7}$ sec.) allows for a rapid scan rate, which in turn results in high operating frequencies (hundreds of cycles/sec.) with a consequent reduction in the 1/f noise of the amplifiers. This also results in a low S/N per interferogram, which facilitates digitization. Since the "Rollin" detector is essentially a photoconductor, it can be ruggedly mounted.

The germanium bolometer is much more difficult to handle since it requires very critical thermal mounting. The Golay cell is much more sensitive to vibration and has lower detectivity than the "Rollin" detector. The Putley detector also has lower detectivity and the additional complication of requiring a magnetic field.

---

1. M.A. Kinch and B.V. Rollin; "Detection of Millimeter and Sub-Millimeter Wave Radiation by Free Carrier Absorption in a Semiconductor"; Brit. J. Appl. Phys., 1963, Vol. 14.

4.2 Mounting and Throughput

Figure 3 is a drawing of the detector assembly. The detector together with its transformer coupling is carried on a stalk. The stalk may be thrust in and out of the liquid helium for convenience in the evaluation of the detector. Cooling of the detector is discussed in Section IV.

The "Rollin" detector is relatively transparent at the .5 mm to 2 mm wavelength range. This, together with the fact that the wavelengths are comparable to the size of the components and detector, makes the method of coupling the detector to the preceding optics an important consideration. By carefully matching the throughput at the detector to that of the rest of the interferometer, the energy gathered by the interferometer is conserved. To accomplish this we will use a multipass device or Spiegelraum to obtain more than one pass through the detector. One possible multipass device is an integrating sphere.

4.3 Detector Signal-to-Noise

The N.E.P. of the detector will be limited by a number of noise sources; the following is a list of the noise sources from which the N.E.P. is determined by the equality, $(N.E.P.)^2 = \Sigma(\Delta W)^2$.

A.) The Johnson noise of the detector: This is given by

$$(\Delta W)^2 = \frac{4kT\ R_c}{S^2}$$

where $k = 1.38 \times 10^{-23}\ J\ {}^\circ K^{-1}$

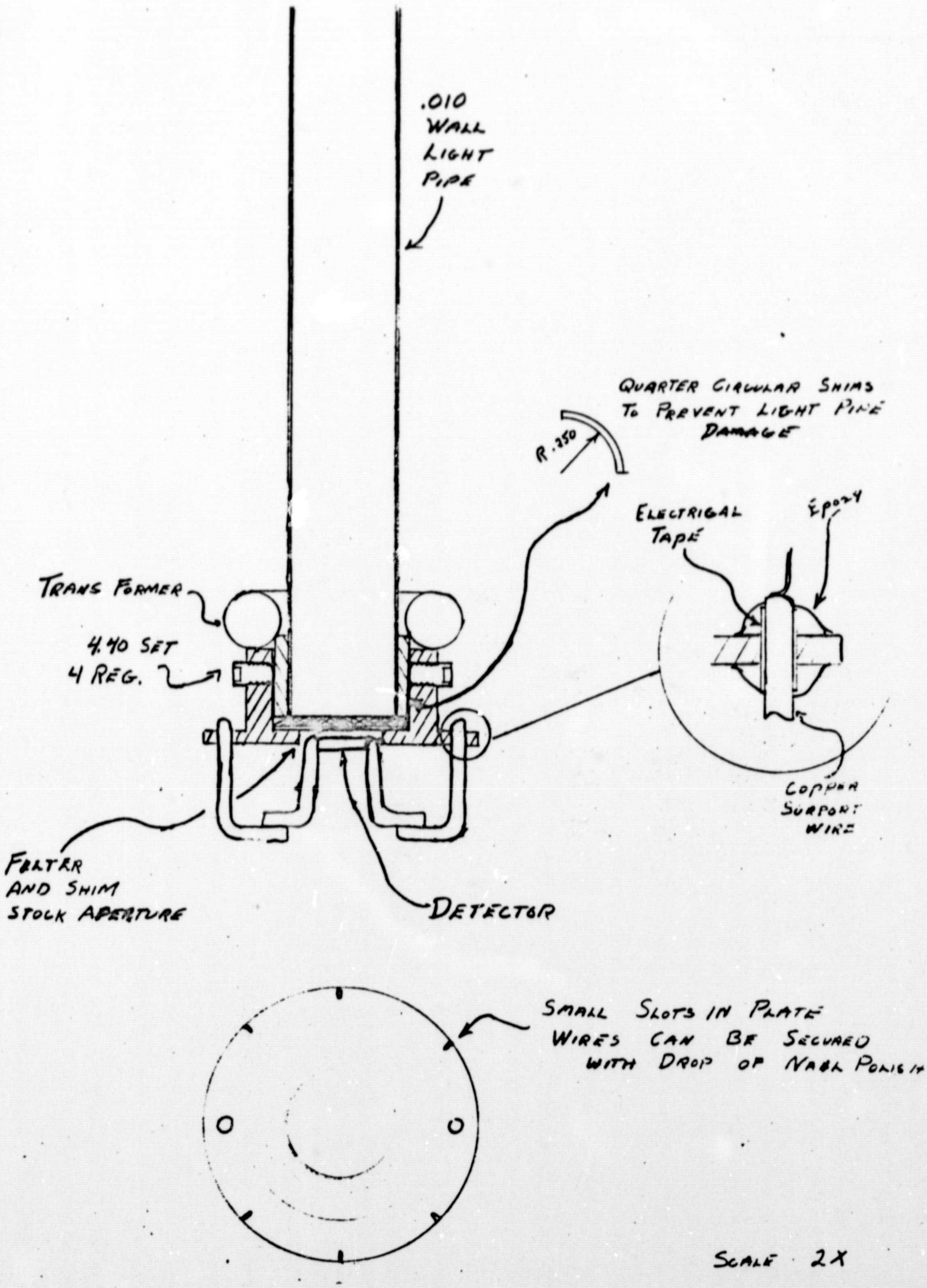

FIGURE 3

SCALE 2X

J COVEY

1/07/66

R_c = detector resistance in ohms

S = responsivity in volts/watt

T = temperature in °K

Calculating for $R_c = 10\Omega$; $S = 100$ v/watt and $T = 4.3$°K, this contribution is

$$(\Delta W)^2 = 5 \times 10^{-26} \text{ watts}^2.$$

B.) The noise resulting from exchange of energy within the lattice: According to Rollin, this is approximately equal to the Johnson noise, or 5×10^{-26} watts^2.

C.) The noise due to the random arrival of photons at the detector: This minimum $(\Delta W)^2$ will depend on the temperature of the spectrometer itself. For a spectrometer temperature of 77°K, and assuming an emissivity $\epsilon = .1$, with a cold shield at liquid helium temperature and limiting the detector f.o.v. to what is required, the photon noise will assume the limiting value:

$$(\Delta W)^2 = (h\nu)^2 N_{eff} ,$$

where N_{eff} is the number of photons over the spectral region of the detector response, h is Planck's constant, and ν is frequency.

Thus

$$N_{eff} \cong \epsilon \int_{\nu_1}^{\nu_2} N_\nu \, d\nu$$

$$\cong 6 \times 10^{12}$$

for

$$\nu_1 = 1.5 \times 10^{11} \text{ cps}$$

$$\nu_2 = 6 \times 10^{11} \text{ cps}$$

Thus

$$(\Delta W)^2 = (h\nu)^2 N_{eff}$$

$$\cong 2.4 \times 10^{-31} \text{watts}^2$$

D.) The noise resulting from the emission of the detector: When the detector is much colder than the source, this noise is negligible.

E.) Amplifier noise: The optimum noise figure for state-of-the-art low noise amplifiers can only be achieved at high source impedances, in the Megohms. For lower source impedances, a matching transformer between the detector and the amplifier is required. By also cooling this transformer to liquid He temperature and operating it in the hundreds of cycles, its noise contribution can be kept small. By cooling a field effect transistor amplifier to liquid nitrogen temperature, an equivalent input noise voltage of about 10^{-8}

volt/cps$^{1/2}$ has been achieved with a negligible shot noise component. So for a transformer ratio of 200/1, an equivalent noise voltage at the detector of $\approx 5 \times 10^{-11}$ v/cps$^{1/2}$ is possible. (or, $(\Delta W)^2 = (\frac{5 \times 10^{-11}}{100})^2 = 2.5 \times 10^{-25}$).

F.) Excess noise like 1/f noise can be minimized by operating at frequencies where this is low.

It is seen from these calculations that only the noise sources A, B, and E are important. Adding these three contributions we get:

$$(N.E.P.)^2 = (5 \times 10^{-26} + 5 \times 10^{-26} + 2.5 \times 10^{-25})^2$$
$$= (3.5 \times 10^{-25})^2$$

or

$$N.E.P. \cong 6 \times 10^{-13} \text{ watts.}$$

While the preamplifier is the main noise source, it is comparable within a factor 2 - 3 to the detector noise.

Another observation is that the radiation noise (C) is much less than the other noise sources, so cooling is unnecessary as far as the noise contribution is concerned. Cooling the optics is thus only necessary in cases where dynamic range in recording is important.

V. Dynamic Range

The following considerations show the influence of the temperature of the interferometer on the dynamic range in the output signal or interferogram.

The energy, P, required at the detector aperture stop for a peak signal-to-RMS noise ratio, S/N, of unity is determined as follows:

$$S/N = 1 = \frac{P\Theta}{N.E.P. \quad \sqrt{n}/t}$$

$$P = \frac{N.E.P. \quad \sqrt{n/t}}{\Theta}$$

Substituting the values -

throughput, $\Theta = .2$ ster - cm^2

$N.E.P. = 6 \times 10^{-13}$ watts

a scan of $n = 800$ resolution elements in time $t = 1$ sec. and a 1 cps bandwidth -

$$P = 8.5 \times 10^{-11} \quad \text{watts/ster - cm}^2$$

Correcting for the interferometer modulation efficiency, $\eta_m = .3$, and collector efficiency $\eta_c = .3$, we find that a source radiance $P \approx 9.5 \times 10^{-10}$ watts/ster-cm^2 is required to give an interferogram with a S/N of unity.

When the detector is cooled and the interferometer is at ambient temperature, 300°K, the self-emission of the instrument will be $P_{.5mm-2mm} = 6.4 \times 10^{-7}$ watts/ster - cm^2. For $\epsilon = .1$, the resulting S/N would be $\frac{6.4 \times 10^{-8}}{9.5 \times 10^{-10}} \approx 68$.

Cooling the interferometer to 77°K with liquid nitrogen will lower its self-emission to $P_{.5mm-2mm} = 3 \times 10^{-8}$ watts/ster-cm^2. Thus, for $\epsilon = .1$, the signal-to-noise ratio in this case is

$$S/N \quad \frac{3 \times 10^{-9}}{9.5 \times 10^{-10}} \approx 3$$

It should be noted that the signal resulting from the instrument's self-emission at ambient temperatures is <u>not</u> of sufficient magnitude to warrant cooling the interferometer for laboratory use; the recording techniques available in the laboratory are such that only the detector need be cooled. However, for rocket and satellite use, where for telemetry, dynamic range presents a problem, a cooled interferometer may be necessary.

VI. Cryogenics

Both the optical system and the detector of the bipath interferometer are cryogenically cooled. The optical cube is cooled with liquid nitrogen, the detector with liquid helium. Figure 4 is a scale drawing of the entire system, showing the location and relative sizes of the separate dewars. Both the liquid nitrogen and the liquid helium are unpumped.

Cooling of the Optical Cube

The interferometer may be cooled to a temperature of 77°K with liquid nitrogen. The capacity of the nitrogen dewar is 4+ liters. The materials of the interferometer components are chosen and designed so as to minimize angular distortions even though the overall size may change appreciably with temperature.

The inside of the interferometer is purged with dry helium so that moving components inside the interferometer are accessible to actuation and adjustments even though the outside of the interferometer is cooled. The interferometer is shown with a crystal quartz window which separates the helium purged interferometer from the liquid nitrogen. The level of the liquid nitrogen in the dewar is maintained by drawing upon an external storage tank.

Cooling of the Detector

The detector and its transformer coupling are cooled with liquid helium. The capacity of the helium dewar is 1 liter.

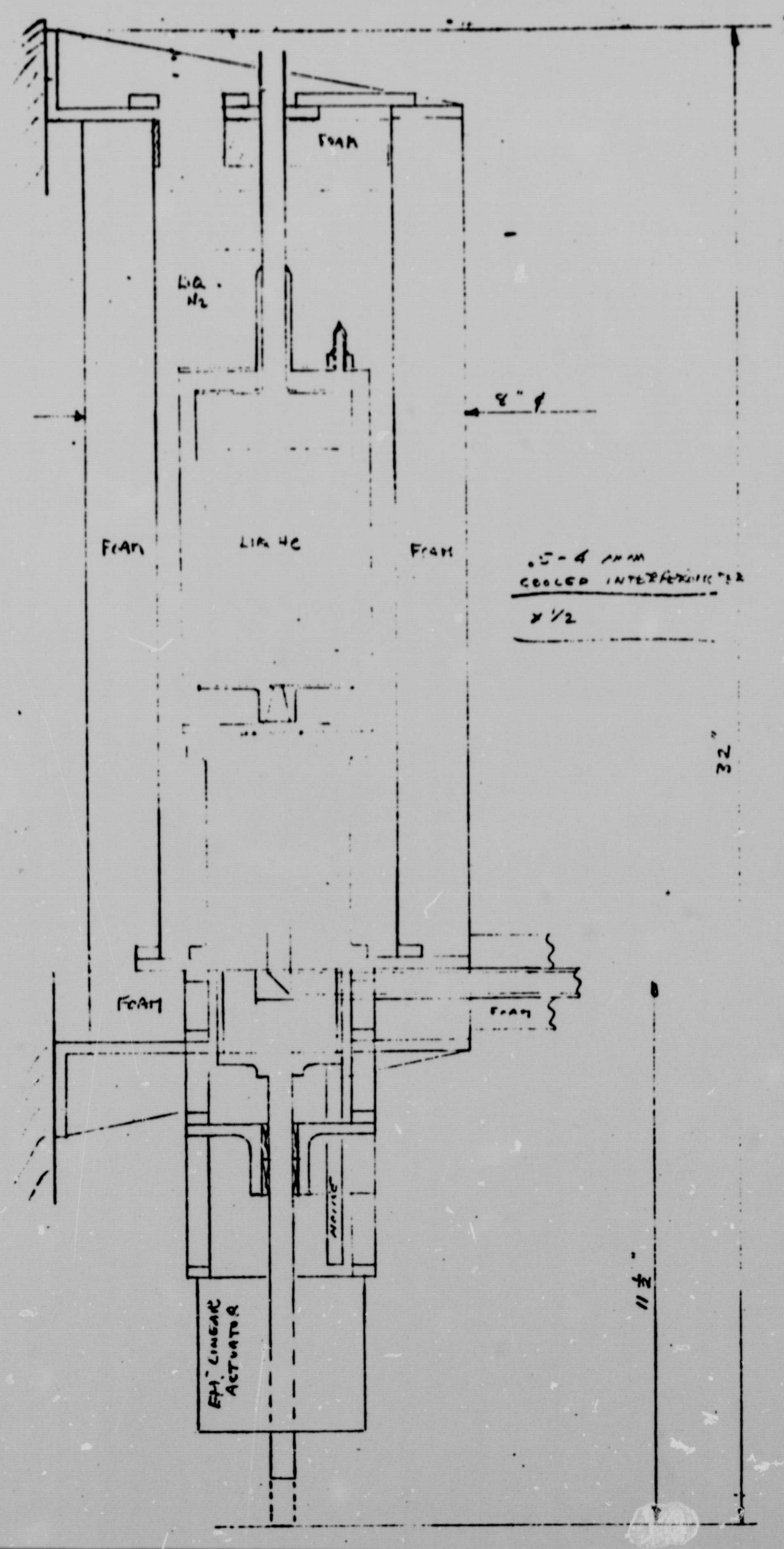
FOAM
LIQ. N2
LIQ HE
FOAM
FOAM
8" ϕ
.5 - 4 mm
COOLED INTERFEROMETER
8 1/2
32"
FOAM
FOAM
11 1/2"
EM. LINEAR ACTUATOR

The temperature of the unpumped helium is 4.3°K. As shown in the drawing, the helium dewar is centrally located inside the nitrogen dewar. Thus, the outside of this dewar is immersed in liquid nitrogen which enables an increase in hold time. The helium is transferred using conventional techniques.

Hold Times

The estimated hold time of the liquid nitrogen is 1 hour; that of the liquid helium is 2 hours.

VII. Electronics

7.1 Detector Preamplifier

The detector signal is amplified by a low noise preamplifier which is impedance matched to the detector. Although the low resistance, 10 ohms, of the "Rollin" detector makes matching to the preamplifier difficult, this is not considered to be a problem.

7.2 Data Handling System

The amplified detector signal is passed through a proper band limiting filter and then recorded in Analog form on a tape recorder. A clock signal derived from the Moiré grating attached to the mirror drive is also recorded. Both these signals are then played back into a Block CO-ADDER. The system is shown the block diagram, Figure 5.

The CO-ADDER is a special purpose time averaging computer which functions to improve the signal-to-noise ratio of spectra. Input interferograms are sampled repeatedly, at a frequency which is more than twice the bandwidth of the signal. The samples are sequentially digitized under control of the clock signal and stored in the core memory. Samples from successive interferograms correspond precisely in mirror position and their levels are digitally added in the memory, so that the coherent signal increases linearly in amplitude with the number of interferograms accumulated. On the other hand, the noise present at the input accumulates, due to its random character, in such a way that the RMS noise power increases with the square root of the number of scans. The resultant gain in signal to noise is thus $\sqrt{n}$, where n is the number of times the same signal is sampled. For example, if the CO-ADDER accumulates as few as 16 interferograms, the S/N will be increased by a factor of four.

The CO-ADDER has a memory capacity of 1024 words; so a maximum of 1024 sample points may be taken on each signal. Each sample is digitized by an 8 bit A/D converter designed to accept a maximum signal of 9 volts, peak to peak. Since the capacity of each word in the memory is 16 bits, it is possible, for example, to co-add up to 256 signals with a 9 volt peak to peak component. Smaller amplitude signals would, of course, be co-added many more times.

After a sufficient number of interferograms have been added in the Co-adder memory, the stored signal may either be played back in Analog form for spectrum analysis, or recorded in digital form on paper or magnetic tape for computer reduction. If the first alternative is adopted, the Analog output of the Co-adder is first processed through a wave analyzer and then recorded on a chart recorder.

The wave analyzer is a narrow-band, variable frequency filter which is slowly tuned over the range of audio frequencies present in the interferogram signal. The wave analyzer accomplishes the inverse Fourier transform of the interferogram; it transforms the interferogram, which is in the time-frequency domain, into the amplitude-frequency domain of the audio frequency spectrum. This audio frequency spectrum can be readily transferred to intensity vs electromagnetic frequency using the calibration information provided with the instrument.

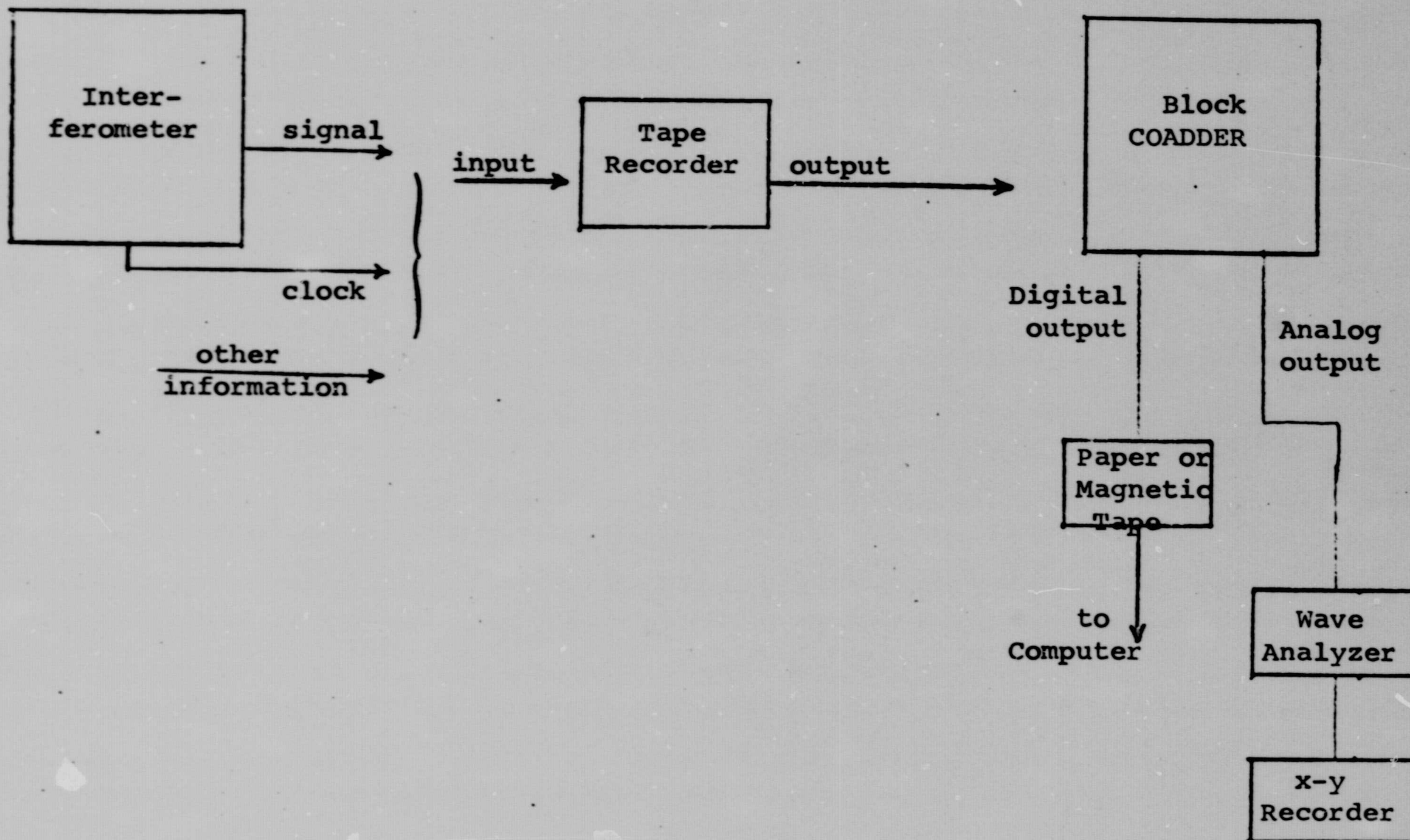

Block Diagram
Bipath Interferometer Spectrometer System

FIGURE 5

VIII. CONCLUSION

The overall design configuration of the Bipath Interferometer Spectrometer, together with calculations which theoretically determine the effectiveness of this instrument for broadband spectral measurements in the .5mm to 2mm wavelength region, has been documented in this report. In the light of these calculations and considerations, Block Engineering believes that fabrication of an operational model of the Bipath Interferometer Spectrometer for geological measurements is certainly warranted. The anticipated signal-to-noise ratio and resolution of the interferometer are more than adequate for passive measurements of the self-radiation of geological samples.